Food Chemistry 396 (2022) 133711

Contents lists available at ScienceDirect

Food Chemistry

journal homepage: www.elsevier.com/locate/foodchem

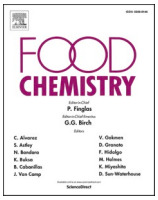

Fluorometric detection of phytase enzyme activity and phosphate ion based on gelatin supported silver nanoclusters

Sanaz Mashhadi Farahani [a], Mehdi Dadmehr [a,*], Mohammad Ali Karimi [b], Behnaz Korouzhdehi [c], Mohammad Amin Karimi [d], Majid Rajabian [a]

[a] Department of Biology, Payame Noor University, Tehran, Iran
[b] Department of Chemistry, Payame Noor University, Tehran, Iran
[c] Department of Biotechnology, College of Agriculture & Natural Resources, University of Tehran, Karaj, Iran
[d] School of Medicine, Shahid Beheshti University of Medical Sciences, Tehran, Iran

ARTICLE INFO

Keywords:
Phytase enzyme
AgNCs
Biosensor
Phosphate
Fluorescence

ABSTRACT

Phytase is the commercial enzyme for bioconversion of phytate substrate to digestible phosphate ions. Recently silver nanoclusters (AgNCs) have received great attention as the optical transducer nanoparticles in biosensors structure. The novel detection platform was developed to detect the phytase enzyme activity and phosphate ions based on fluorescence quenching of AgNCs. The AgNCs were synthesized through gelatin supported reaction and characterized by TEM, FTIR and XRD analysis. The hydrolytic effect of phytase enzyme and subsequent phosphate release led to suppression of AgNCs fluorescence. The linear range was observed for enzyme in the range of 0.5–5 U/mL with the detection limit of 0.2 U/mL. Also, the same fluorescence quenching effect was observed in the presence of phosphate ion in the linear range of 1 to 16 μM with a detection limit of 0.5 μM. The proposed mechanism showed effectiveness of detection strategy for detection of phytase enzyme and phosphate ion.

1. Introduction

Phosphate is regarded as one of the most limiting nutrients for animals in the form of phytate (myo inositol (1,2,3,4,5,6) hexakisphosphate) which present in the feeding plants. The monogastric animals are incapable of digesting the phytate which reduces the uptake of many minerals and is considered as the antinutrient factor (Shanmugam, 2018). Most of the absorbed phosphate in plant storage parts such as seeds, grains, and cereals are immobilized in phytate structure. Phytase is a phosphomonoester hydrolase enzyme used to eliminate anti-nutrients in plant-based feeds. The unavailability of phytate contents originated from the lack of phytase enzyme in the digestive system of many organisms, including human and monogastric livestock (Kumar, Sangwan, Verma, & Agrawal, 2014; Zhang, Yang, Xie, Gao, Bai, Zhang, et al., 2020). To overcome this problem, inorganic phosphate is supplemented in animal diets for compensation of phosphate deficiency. The presence of residual extra and unabsorbed phosphate and phytate causes serious environmental pollution (Tan, Miao, Liu, Cao, Wu, Xie, et al., 2016; Zhang, et al., 2020). Phytic acid content is about 1 %–5% in legumes, cereals, oilseeds, and nuts (Singh, 2017a, 2017b; Singh & Satyanarayana, 2011a, 2011b). Interaction of phytate with other proteins forms the complexes under acidic and alkaline pH conditions which have adverse effect on proteins structure and their proteolytic digestibility (Vashishth, Ram, & Beniwal, 2017; Yao, Zhang, Lu, Hu, Wang, & Liang, 2012). In addition, phytate is a strong anti-nutrient since it can chelate mineral cation elements (Ca^{2+}, Mg^{2+}, Fe^{2+}, Zn^{2+}), starch and proteins, and make these nutrients less available to animals (Haefner, Knietsch, Scholten, Braun, Lohscheidt, & Zelder, 2005; Shanmugam, 2018).

The addition of Phytases is widely applied in animal nutrition to facilitate phytate hydrolysis and dephosphorylation (Nováková, Vértesi, Béres, Petkov, Niederberger, Van Gaver, et al., 2021). Phytase hydrolysis process leads to release of myo-inositol and inorganic phosphates (P), which eliminate its antinutritional properties (Rao, Rao, Reddy, & Reddy, 2009). Also, the hydrolytic process results in the inhibition of undesirable chelating property of metal ions by phytate (Singh, Boukhris, Kumar, Yadav, Farhat-Khemakhem, Kumar, et al., 2020). There is great industrial demand for phytase enzymes with higher proteolytic and thermal stabilities which are durable under high temperatures at the steaming and pelleting steps in the feed production process

* Corresponding author.
E-mail address: mdadmehr@pnu.ac.ir (M. Dadmehr).

https://doi.org/10.1016/j.foodchem.2022.133711
Received 11 March 2022; Received in revised form 8 July 2022; Accepted 12 July 2022
Available online 16 July 2022

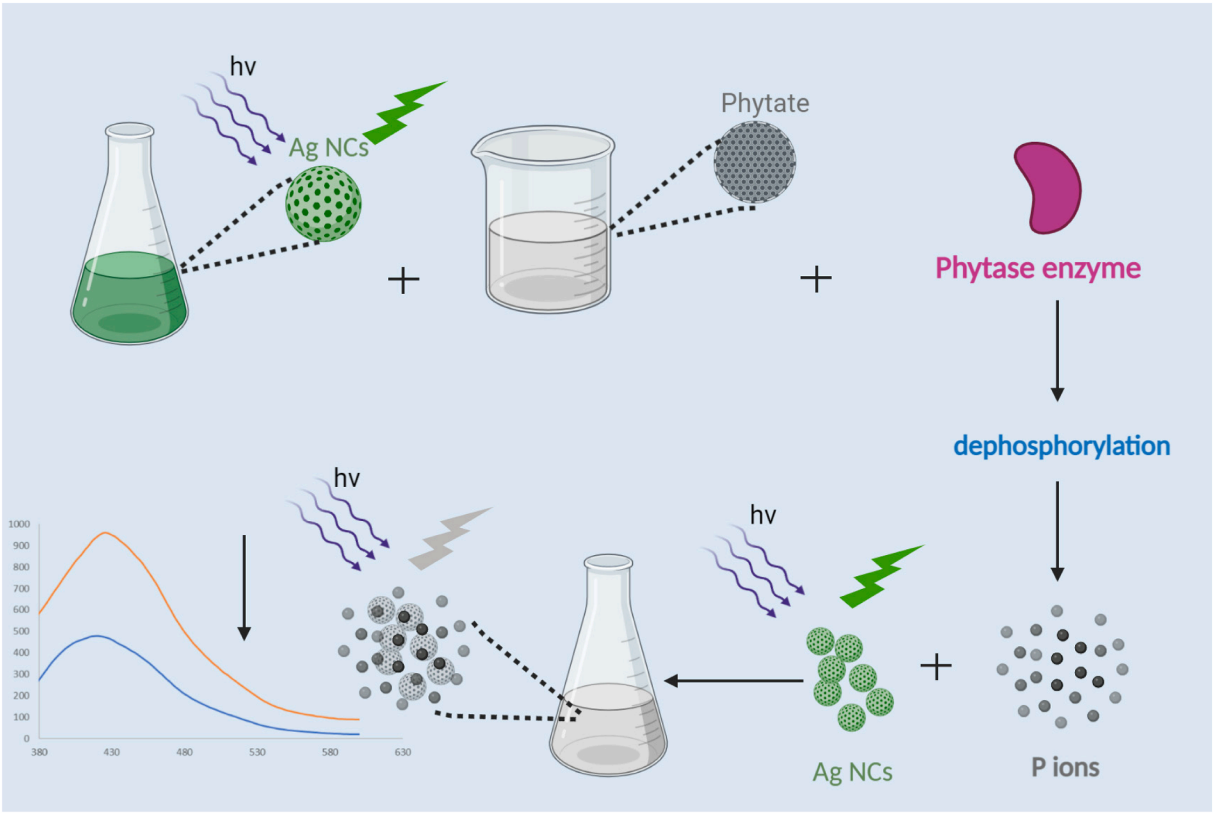

Scheme 1. Schematic illustration of proposed mechanism for detection of phytase enzyme and phosphate ion.

and in the digestive tract of animals (Tan, et al., 2016; Zhang, et al., 2020).

So far, several phosphates analysis-based methods have been developed for the detection of phytase activity (Nuobariene, Cizeikiene, Gradzeviciute, Hansen, Rasmussen, Juodeikiene, et al., 2015; Qvirist, Carlsson, & Andlid, 2015; Sanikommu, Pasupuleti, & Vadalkonda, 2014), which most of them are considered as rapid and efficient approaches. Some studies (Carlsson, Bergman, Skoglund, Hasselblad, & Sandberg, 2001; Türk, Sandberg, Carlsson, & Andlid, 2000) determined the phytase activity by analyzing IP6 concentration using high-performance liquid ion chromatography (HPLC). Most of recently applied colorimetric phosphate analysis methods (Caputo, Visconti, & De Angelis, 2015; Sanikommu, Pasupuleti, & Vadalkonda, 2014) were based on the conventional presented method by Fiske and Subbarow (Fiske & Subbarow, 1925). In this method, ammonium molybdate solution was added to a phosphate-containing sample, which resulted in formation of yellow phosphomolybdic acid and following reduced by 1-amino-2-naphtol-4-sulfonic acid (ANSA) to molybdenum blue. Since ANSA is toxic and also has a multistep solution preparation reaction, alternative methods have been developed to exclude ANSA. One approach was developed based on colorimetric detection of the formed yellow phosphomolybdic acid without reduction step to molybdenum blue (Greiner, Jany, & Alminger, 2000; Nuobariene, et al., 2015). In another studies, the ANSA was exchanged with the different agents as the reducing factor such as ferrous sulfate (Bae, Yanke, Cheng, & Selinger, 1999; Qvirist, Carlsson, & Andlid, 2015), stannous chloride (Dickman & Bray, 1940) or ascorbic acid (Katewa & Katyare, 2003) to produce molybdenum blue. Another commonly used method for detection of phytase activity is the molybdenum yellow method (Freund, Mayr, Tietz, & Schultz, 1992) and the ferrous sulfate molybdenum blue method (Greiner, Jany, & Alminger, 2000). Recently, a novel platform based on biosensors were also established to detect the phytase enzyme (Mak, Ng, Chan, Kwong, & Renneberg, 2004; Shi, Chen, & Niu, 2021).

Biosensors are regarded as the detection platform for monitoring and determination of biological analyte detection. Several nanostructures have been applied in biosensors platforms to improve their sensitivity toward biological analytes (Cheraghi Shahi et al., 2021; Karimi et al., 2019; Mortezaei et al., 2021; Rafiei et al., 2019). Silver nanoclusters (AgNCs) present significant potential for biosensing and bioimaging due to their tunable and efficient fluorescence properties and also showed lower toxicity and size in comparison with conventional quantum dots (Dadmehr, Karimi, & Korouzhdehi, 2020; Díez & Ras, 2011; Xie, Shen, Duan, Han, Zhang, & Lu, 2020). One of the major limitations in bio-applications of AgNCs is their high tendency to irreversible aggregation, which originated from their high surface energy. To overcome this challenge, many attempts have been made to synthesize stable AgNCs using a variety of ligands, such as short thiols (Cathcart, Mistry, Makra, Pietrobon, Coombs, Jelokhani-Niaraki, et al., 2009; Zheng, Yuan, & Xie, 2017), oligonucleotides (Dadmehr, Hosseini, Hosseinkhani, Ganjali, & Sheikhnejad, 2015; Han & Wang, 2011), peptides (Adhikari & Banerjee, 2010; Díez, Hahn, Ikkala, Börner, & Ras, 2010) and polymers (Li, Chen, Luo, & Li, 2013; J. Zhang, Xu, & Kumacheva, 2005). In the present method we fabricated novel biosensing approach toward the detection of both phytase enzyme and phosphate ions. The gelatin-mediated silver nanoclusters were used as the detection probe in the present study. The obtained results showed that the addition of phytase enzyme in the presence of phytate as the substrate resulted in fluorescence quenching of silver nanoclusters which was dependent on enzyme activity (Scheme 1). The same behavior was obtained after phosphate ion addition and the applied method showed efficient response for phosphate detection. It was concluded that fluorescence quenching resulted from the interaction of released phosphate with silver nanoclusters which was correspondent to phytase enzyme activity. The applied method was facile and efficient for quantitative detection of phytase enzyme and soluble phosphate ions.

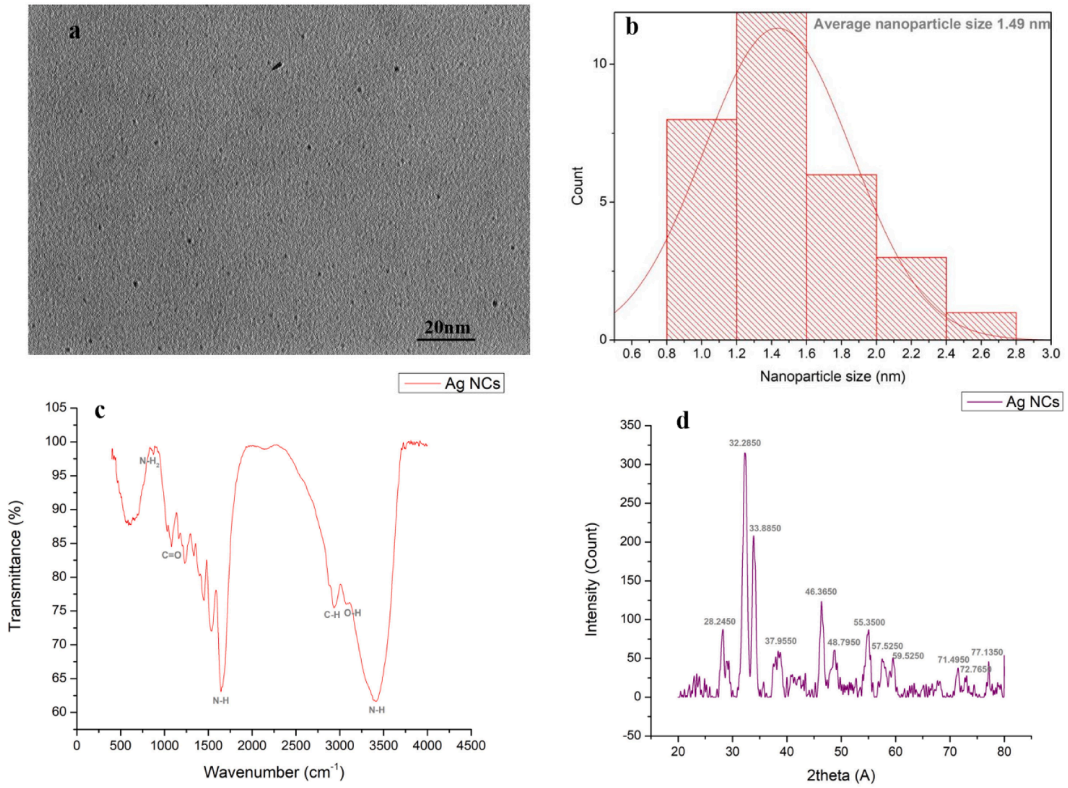

Fig. 1. a) TEM image of synthesized AgNCs by gelatine, b) size distribution of AgNCs, c) FTIR spectrum of AgNCs and d) XRD analysis of prepared AgNCs.

2. Materials and methods

2.1. Reagents and materials

Rice bran was purchased from a local supermarket, in Mashad, Iran. Acetone, hydrochloric acid, barium hydroxide, sodium hydroxide, EDTA, ammonium heptamolybdate tetrahydrate, sodium vanadate and nitric acid were purchased from Merck. Sulphuric acid, sodium acetate and calcium chloride and phytase were prepared from Sigma-Aldrich. Other chemicals include $HAuCl_4$, Trisodium citrate, Ascorbic acid, Gelatin, $AgNO_3$, acetic acid, NaCl, $AlCl_3$, CuSo4, $FeCl_3.6H_2O$, $C_4H_{10}O_6Zn$, KI, Na_2HPO_4 were purchased from Merck and Acros.

2.2. Synthesis of gelatin-based AgNCs (Gelatin/AgNCs)

For the preparation of AgNCs nanostructures we used gelatin as the substrate, for synthesis of AgNCs. Briefly, 5 mg gelatin was dissolved in 20 mL distilled water while the solution pH was adjusted to 7. To prepare the homogenous solution of gelatin substrate the reaction temperature was adjusted to 55 °C. Then $AgNO_3$ solution containing 0.0017 g was added to the reaction and shaken vigorously for 5 min and finally transferred on the magnet stirrer, followed by incubation in the dark at 40 °C overnight. The obtained AgNCs were stored in dark condition at 4 °C for further analysis and experiments.

2.3. Characterization of AgNCs

The characterization of synthesized AgNCs structure was performed by TEM, FTIR and XRD analysis. The TEM analysis was performed using TEM (ZEISS- AB LEO912) operated at 120 kV to determine the size and shape of AgNCs. In order to determine the surface functional group over synthesized AgNCs, FTIR analysis was investigated by FT-IR spectrometer (Shimadzu-8400, Japan). The X-ray diffraction pattern was also obtained through X-ray diffraction device (XRD, Philips analytical diffractometer).

2.4. Spectroscopic analysis

The spectroscopic analysis of prepared AgNCs was performed to determine their UV–Visible absorbance and fluorescence spectra throughout the experiment. UV–vis spectrophotometer (Shimadzu, double beam, Japan) was used for analysis of absorbance spectra. The fluorescence emission spectra of performed reactions were obtained at the excitation of 350 nm with the silt widths of 5 nm. Analysis was also done by PerkinElmer LS 45 Luminescence spectrometer.

2.5. Detection of phytase enzyme and phosphorous ions

To detect phytase enzyme, the phytate as the substrate was used to provide the efficient enzyme reaction condition. So. 16.8 mg of phytate was dissolved in 0.5 mL distilled water and subsequently, 1 mL of gelatin/AgNCs was added to the reagent bottle and they were mixed at room temperature. Then serial dilution of phytase solution concentrations were added to the obtained reaction and incubated for 2 h at 37 °C to carry out the hydrolysis enzyme reaction. Then fluorescence intensities of obtained solutions were recorded. For optimization of detection performance, pH values of the solutions were measured and adjusted by HCl (0.1 M) NaOH (0.1 M) to prepare the reactions with pH 4 to 12, respectively.

3. Results and discussion

3.1. Proposed mechanism

The proposed mechanism for detection of phytase enzyme activity is illustrated in Scheme 1. Fabrication of the detection platform was performed through the gelatin-based synthesis of AgNCs. The synthesized AgNCs showed green-emitting fluorescence at 420 nm. The presence of

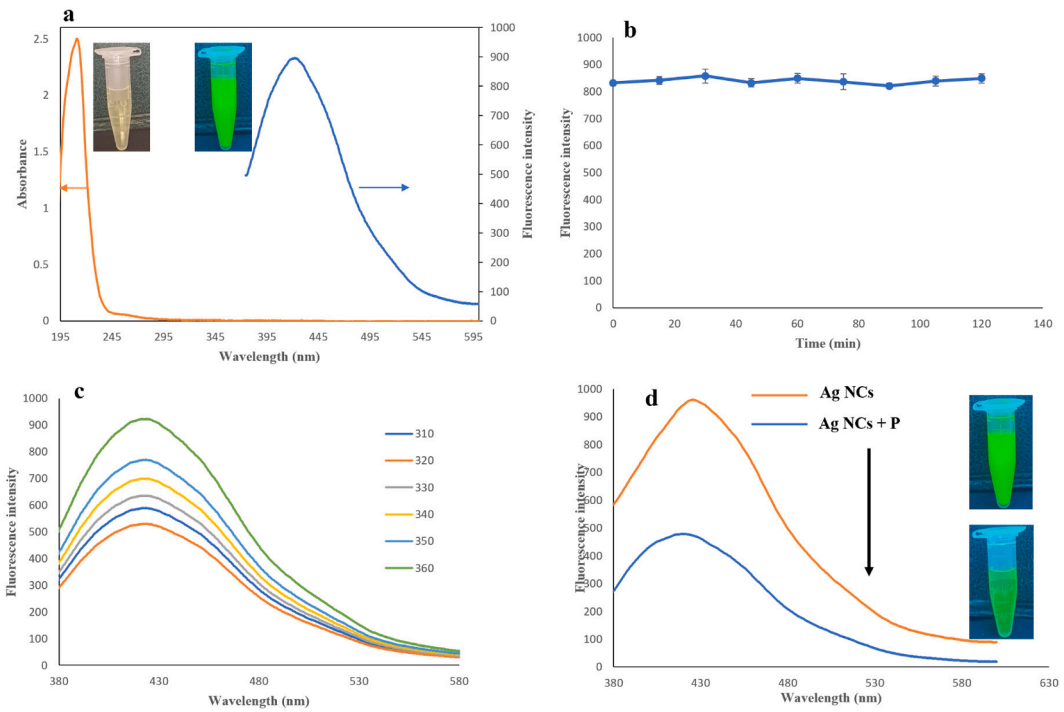

Fig. 2. a) UV– visible absorption and fluorescence spectra of AgNCs, inset shows the AgNCs solution under visible light and UV irradiation, b) stability of AgNCs under different incubation time c) fluorescence intensity of AgNCs by different excitation wavelength d) fluorescence quenching of AgNCs after addition of phosphate ion solution, inset shows the samples under UV light irradiation.

phytate as the enzyme substrate and enzymatic activity of phytase enzyme resulted in phosphate ions release in the solution. Released phosphate ions could interfere with AgNCs emission and result in fluorescence quenching which corresponded to enzyme activity. We concluded that phosphate ions could interact with the functional groups and ligands on the surface of AgNCs, reducing the stability of the self-assembled structure of the original AgNCs. Another possible mechanism would be based on electron transfer between AgNCs and phosphate ions. After excitation of AgNCs the excited electrons move from the valence band to the conduction band of AgNCs. When the electrons relax to their valence band with a lower energy level, energy is released as a photon and fluorescence emission. In the presence of phosphate ions, the excited electrons can enter the unfilled d orbital of P, then led to fluorescence quenching of AgNCs.

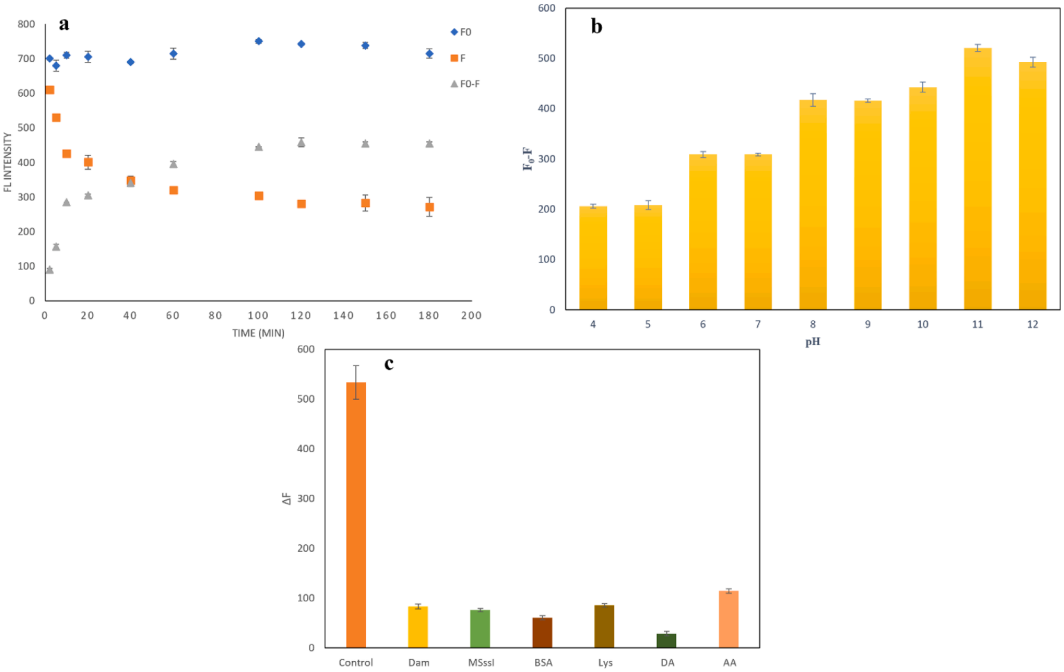

Fig. 3. a) Effect of reaction incubation time on the efficiency and fluorescence intensity of applied method, b) effect of different pH values on the fluorescence intensity of AgNCs in the assay, c) selectivity of method by effect of non-specific enzymes and molecules on fluorescence intensity of AgNCs.

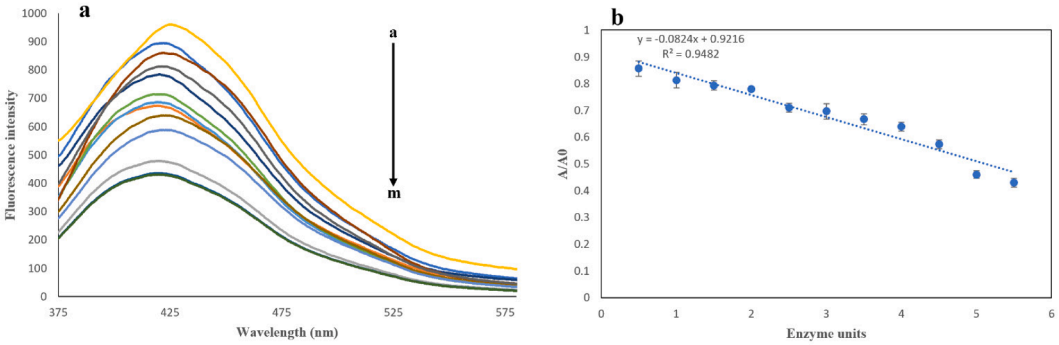

Fig. 4. a) Effect of different concentration of applied phytase enzyme on fluorescence intensity of AgNCs in the range of 0.5 – 5 U/mL, b) plot for the fluorescence intensity versus the concentration of applied enzyme.

3.2. Characterization of synthesized Gelatin/AgNCs

For the determination of synthesized gelatin/AgNCs morphology and size, the TEM analysis was performed. The obtained results showed that the prepared AgNCs have round shape morphology (Fig. 1a). The particle size distribution histogram indicated the formation of AgNCs with a size of about 1–3 nm and with a mean diameter of 1.49 nm (Fig. 1b). The X-ray diffraction pattern (XRD) of synthesized silver nanoclusters was determined and obtained pattern showed that the AgNCs have good crystallinity (Fig. 1d). The characteristic XRD peak for AgNCs appeared at 28.245°, 32.2850°, 33.8850°, 46.3650°, 55.0350°, 57.5250°, 59.5250°, 71.4950°, 72.7650°, 77.1350°, that corresponds to the planes with miller indices of (1 1 1), (2 0 0), (2 2 0), (3 1 1), (2 2 2), (4 0 0), (3 3 1), (4 2 0), (4 2 2), (5 1 1) and (4 4 0) respectively. These peaks were matched with the face-centered cubic (fcc) structure of silver (JCPDS file No. 04–0783). FTIR spectroscopy analysis provided information about the local molecular environment of the organic molecules on the surface of nanocluster. As shown in Fig. 1e, the observed peaks at 3324.74 and 1660 cm^{-1} correspond to N—H stretching and bending vibrations. Peaks at 2880.36 and 1118.70 correspond to -C—H and -C═O, respectively. The peaks 3076.50 cm^{-1} and 2945.12 cm^{-1} are assigned to OH stretching and aldehydic C—H stretching, respectively. The weaker band at 1660 cm^{-1} corresponds to amide I arising due to carbonyl stretch in proteins.

3.3. Spectroscopy properties of AgNCs

The UV–Visible absorption spectrum of AgNCs showed λ^{max} around 200 nm and the maximum fluorescence emission wavelength was located at 420 nm. Also, the prepared solution was yellow under visible light and emitted green fluorescence under UV light irradiation (Fig. 2a). For determination of stability of prepared AgNCs, the fluorescence emission at 400 nm was determined every 15 min for a while. As shown in Fig. 2b, the fluorescence intensities did not show significant changes during the time of 120 min. So, it was concluded that the AgNCs show good stability in time intervals. As shown in Fig. 2c, no fluorescence spectra shift was observed under different excitation wavelengths but the fluorescence intensities were affected by excitation change. The synthesized AgNCs showed the highest fluorescence emission in the wavelength of 420 nm at the excitation of 350 nm. As illustrated in Fig. 2d quenching effect of phosphate on fluorescence intensity of AgNCs was observed after the addition of phosphate ion, which confirmed that the AgNCs could act as the probe for determination of released phosphate in reaction.

3.4. Optimization of enzyme detection condition

For further optimization, the effect of time incubation on reaction was investigated. As shown in Fig. 3a, the fluorescence intensity difference ($\Delta F = F_0$-F) of assay reaction was determined where the F_0 was the initial fluorescence intensity and F was the fluorescence intensity after the performed reaction. The obtained results showed little and gradual decrease after incubation for 2 h. After that, the fluorescence change was constant for another 1 h and subsequently 2 h was determined as the optimum reaction time. Following, effect of different pH values on the reaction performance was determined (Fig. 3b). Preparation of reaction solutions with adjustment of several pH values showed the best performance in fluorescence emission difference (F_0-F) at alkaline pH at 11 with the highest fluorescence quenching. However, other applied pH also resulted to fluorescence quenching but it was not as well as alkaline pH. It has been demonstrated that phytase enzyme showed considerable pH adaptability (Zhang, Wu, Ng, Chen, & Wang, 2013). Then, we assumed that the obtained result may originated from interaction between released phosphate and synthesized AgNCs. The alkaline pH condition resulted to more phosphate ion interaction with synthesized AgNCs and led to the significant fluorescence detection performance. So, pH 11 was selected as the optimum pH to adjust the reaction solution through the enzyme detection approach.

3.5. Measurement of phytase enzyme activity

As illustrated in Fig. 4a with increasing of phytase enzyme concentration, the fluorescence intensity of AgNCs decreased in linear range. The observed results were consistent with our explained hypothesis and the released phosphor ions interacted with AgNCs and induced the AgNCs changes which caused fluorescence quenching. The highest fluorescence emission was related to bare AgNCs emission and the other quenched fluorescence spectra were observed after the addition of phytase enzyme in the range of 0.5 – 5 U/mL enzyme concentrations (Fig. 4b). Moreover, the assay results showed that the fluorescence emission wavelength has a good linear relationship versus the addition of enzyme concentration in a certain range. The fluorescence of the applied reaction decreased gradually after addition of enzyme concentration. In the presented graph, F_0 is the fluorescence intensity of reaction at 420 nm before incubation with phytase enzyme, while the F represents the fluorescence intensity of reaction after the addition of enzyme concentration. The corresponding equation was $Y = -0.0824x + 0.9216$ ($R^2 = 0.92$), where Y was the fluorescence intensity and the × was phytase enzyme concentration. The limit of detection is determined to be 0.2 U/mL. The obtained results were compared with the previously published studies in Table S1. The calculated linear range and limit were comparable to other studies and showed the efficient performance of our applied method. So, according to obtained results, the detection platform was confirmed for fluorometric detection of phytase enzyme in applied reaction.

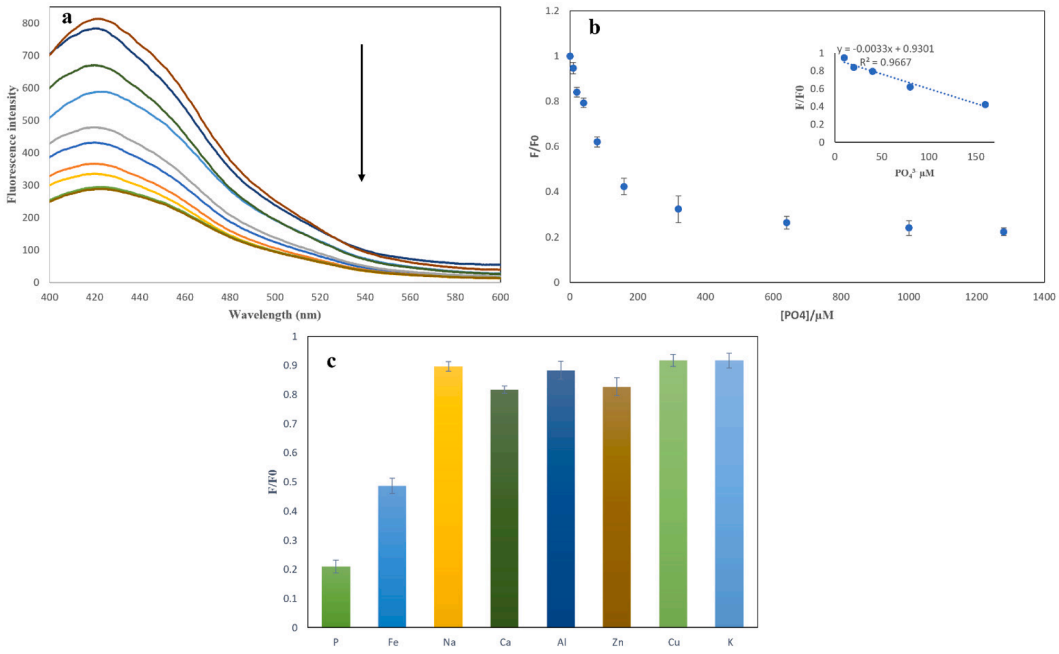

Fig. 5. a) Fluorescence spectra of AgNCs after addition of different concentration of phosphate ions, b) plot of fluorescence intensity of AgNCs versus different concentration of applied phosphate ion, c) selectivity of phosphate ion detection approach by addition and comparison of other ions.

3.6. Selectivity of enzyme detection approach

In order to determine the selectivity of the performed experiment, non-specific enzymes, proteins and small molecules including Dam methyltransferase enzymes, MSss1 methyltransferase enzyme (1U/mL), bovine serum albumin (BSA) 10 μg/mL, lysozyme (Lys), dopamine (DA) and ascorbic acid have been applied. The phytase enzyme was used at the same time as the control sample. As presented in Fig. 3c, other applied agents showed negligible effect on the assay fluorescence difference (ΔF) which illustrated the efficient selectivity of the applied method.

3.7. AgNCs mediated detection of phosphate ion

We performed the experiment upon release of phosphorus ion and its quenching effect on fluorescence emission. So, the effect of PO_4^{3-} concentration was investigated in the following experiment. Different concentrations of PO_4^{3-} were applied to determine the induced changes in fluorescence intensity of AgNCs. As shown in Fig. 5a with increase of PO_4^{3-} ion, the fluorescence intensity was decreased gradually (from 0 to 1400 μM/L) and also corresponding plot indicated that the F/F_0 had a good linear relationship with PO_4^{3-} ion concentration in the range of 1–16 μM (inset of Fig. 5b). The higher concentration didn't make a significant change in fluorescence intensity. The equation of calibration curve was $F = -0.003x + 0.93$ ($R^2 = 0.96$) and LOD of proposed biosensor for detection of phosphorous was calculated at 0.5 μM/L.

3.8. Selectivity of phosphate ion detection

To compare and determine the effect of other ions, the same concentration of several ions has been applied in the assay solution. As illustrated in Fig. 5c, the obtained results showed that the highest quenching effects were resulted from the effect of PO_4^{3-} and Fe^{3+} ions. The interaction of other inorganic cations including Na^+, Ca^{2+}, Al^{3+}, Zn^{2+}, $Cu^{2+}$and K^+ showed they would not interfere in the detection system. The results illustrated that our approach has higher sensitivity and response to PO_4^{3+} ions.

4. Conclusion

In summary, a fluorescence-based method was developed for sensitive detection of phytase enzyme activity and phosphate ion detection. The enzymatic activity of phytase enzyme in the presence of phytate as the substrate led to release of phosphate ions and subsequently resulted to fluorescence quenching of gelatin prepared AgNCs. The addition of phosphate ions also decreased the fluorescence intensity of AgNCs in the linear range. The quenching effect of AgNCs induced through their interaction with phosphate ions and provided low detection limit for phytase enzyme and phosphate detection. The proposed strategy showed advantages including facile synthesis, high sensitivity and selectivity and fast response. The high sensitivity of this method also presents its practical applications in different enzyme and ion detection strategies.

CRediT authorship contribution statement

Sanaz Farahani Mashhadi: Investigation. **Mehdi Dadmehr:** Supervision, Writing – review & editing. **Mohammad Ali Karimi:** . **Behnaz Korouzhdehi:** Formal analysis, Resources. **Mohammad Amin Karimi:** Formal analysis. **Majid Rajabian Noghondar:** Validation.

Declaration of Competing Interest

The authors declare that they have no known competing financial interests or personal relationships that could have appeared to influence the work reported in this paper.

Data availability

No data was used for the research described in the article.

Appendix A. Supplementary data

Supplementary data to this article can be found online at https://doi.org/10.1016/j.foodchem.2022.133711.

References

Adhikari, B., & Banerjee, A. (2010). Short-peptide-based hydrogel: A template for the in situ synthesis of fluorescent silver nanoclusters by using sunlight. *Chemistry–A. European Journal, 16*(46), 13698–13705.

Bae, H., Yanke, L., Cheng, K.-J., & Selinger, L. (1999). A novel staining method for detecting phytase activity. *Journal of Microbiological Methods, 39*(1), 17–22.

Caputo, L., Visconti, A., & De Angelis, M. (2015). Selection and use of a Saccharomyces cerevisae strain to reduce phytate content of wholemeal flour during bread-making or under simulated gastrointestinal conditions. *LWT-Food Science and Technology, 63*(1), 400–407.

Carlsson, N.-G., Bergman, E.-L., Skoglund, E., Hasselblad, K., & Sandberg, A.-S. (2001). Rapid analysis of inositol phosphates. *Journal of Agricultural and Food Chemistry, 49*(4), 1695–1701.

Cathcart, N., Mistry, P., Makra, C., Pietrobon, B., Coombs, N., Jelokhani-Niaraki, M., & Kitaev, V. (2009). Chiral thiol-stabilized silver nanoclusters with well-resolved optical transitions synthesized by a facile etching procedure in aqueous solutions. *Langmuir, 25*(10), 5840–5846.

Dadmehr, M., Hosseini, M., Hosseinkhani, S., Ganjali, M. R., & Sheikhnejad, R. (2015). Label free colorimetric and fluorimetric direct detection of methylated DNA based on silver nanoclusters for cancer early diagnosis. *Biosensors and Bioelectronics, 73*, 108–113.

Dadmehr, M., Karimi, M. A., & Korouzhdehi, B. (2020). A signal-on fluorescence based biosensing platform for highly sensitive detection of DNA methyltransferase enzyme activity and inhibition. *Spectrochimica Acta Part A: Molecular and Biomolecular Spectroscopy, 228*, Article 117731.

Dickman, S., & Bray, R. (1940). Colorimetric determination of phosphate. *Industrial & Engineering Chemistry Analytical Edition, 12*(11), 665–668.

Díez, I., Hahn, H., Ikkala, O., Börner, H. G., & Ras, R. H. (2010). Controlled growth of silver nanoparticle arrays guided by a self-assembled polymer–peptide conjugate. *Soft Matter, 6*(14), 3160–3162.

Díez, I., & Ras, R. H. (2011). Fluorescent silver nanoclusters. *Nanoscale, 3*(5), 1963–1970.

Fiske, C. H., & Subbarow, Y. (1925). The colorimetric determination of phosphorus. *Journal of Biological Chemistry, 66*(2), 375–400.

Freund, W. D., Mayr, G. W., Tietz, C., & Schultz, J. E. (1992). Metabolism of inositol phosphates in the protozoan Paramecium: Characterization of a novel inositol-hexakisphosphate-dephosphorylating enzyme. *European Journal of Biochemistry, 207*(1), 359–367.

Greiner, R., Jany, K.-D., & Alminger, M. L. (2000). Identification and properties of myo-inositol hexakisphosphate phosphohydrolases (phytases) from barley (Hordeum vulgare). *Journal of Cereal Science, 31*(2), 127–139.

Haefner, S., Knietsch, A., Scholten, E., Braun, J., Lohscheidt, M., & Zelder, O. (2005). Biotechnological production and applications of phytases. *Applied Microbiology and Biotechnology, 68*(5), 588–597.

Han, B., & Wang, E. (2011). Oligonucleotide-stabilized fluorescent silver nanoclusters for sensitive detection of biothiols in biological fluids. *Biosensors and Bioelectronics, 26*(5), 2585–2589.

Katewa, S. D., & Katyare, S. S. (2003). A simplified method for inorganic phosphate determination and its application for phosphate analysis in enzyme assays. *Analytical Biochemistry, 323*(2), 180–187.

Kumar, V., Sangwan, P., Verma, A., & Agrawal, S. (2014). Molecular and biochemical characteristics of recombinant β-propeller Phytase from Bacillus licheniformis strain PB-13 with potential application in aquafeed. *Applied Biochemistry and Biotechnology, 173*(2), 646–659.

Li, B. L., Chen, J. R., Luo, H. Q., & Li, N. B. (2013). Electrocatalytic activity of polymer-stabilized silver nanoclusters for hydrogen peroxide reduction. *Journal of Electroanalytical Chemistry, 706*, 64–68.

Mak, W. C., Ng, Y. M., Chan, C., Kwong, W. K., & Renneberg, R. (2004). Novel biosensors for quantitative phytic acid and phytase measurement. *Biosensors and Bioelectronics, 19*(9), 1029–1035.

Nováková, J., Vértesi, A., Béres, E., Petkov, S., Niederberger, K. E., Van Gaver, D., … Balázs, Z. (2021). Safety assessment of a novel thermostable phytase. *Toxicology Reports, 8*, 139–147.

Nuobariene, L., Cizeikiene, D., Gradzeviciute, E., Hansen, Å. S., Rasmussen, S. K., Juodeikiene, G., & Vogensen, F. K. (2015). Phytase-active lactic acid bacteria from sourdoughs: Isolation and identification. *LWT-Food Science and Technology, 63*(1), 766–772.

Qvirist, L., Carlsson, N.-G., & Andlid, T. (2015). Assessing phytase activity. *Journal of Biological Methods, 2*(1), e16–e.

Rao, D., Rao, K., Reddy, T., & Reddy, V. (2009). Molecular characterization, physicochemical properties, known and potential applications of phytases: An overview. *Critical Reviews in Biotechnology, 29*(2), 182–198.

Sanikommu, S., Pasupuleti, M., & Vadalkonda, L. (2014). Comparison of phosphate estimating methods in the presence of phytic acid for the determination of phytase activity. *Preparative Biochemistry and Biotechnology, 44*(3), 231–241.

Shanmugam, G. (2018). Characteristics of phytase enzyme and its role in animal nutrition. *International Journal of Current Microbiology and Applied Sciences, 7*(3), 1006–1013.

Shi, H., Chen, L., & Niu, N. (2021). An off-on fluorescent probe based on graphene quantum dots intercalated hydrotalcite for determination of ascorbic acid and phytase. *Sensors and Actuators B: Chemical, 345*, Article 130353.

Singh, B. (2017a). Free and immobilized Aspergillus oryzae SBS50 producing protease-resistant and thermostable phytase. *3. Biotech, 7*(3), 1–8.

Singh, B. (2017b). Purification and characterization of a protease-resistant phytase of Aspergillus oryzae SBS50 whose properties make it exceptionally useful as a feed supplement. *International Journal of Biological Macromolecules, 103*, 458–466.

Singh, B., Boukhris, I., Kumar, V., Yadav, A. N., Farhat-Khemakhem, A., Kumar, A., Singh, D., Blibech, M., Chouayekh, H., & Alghamdi, O. A. (2020). Contribution of microbial phytases to the improvement of plant growth and nutrition: A review. *Pedosphere, 30*(3), 295–313.

Singh, B., & Satyanarayana, T. (2011a). Microbial phytases in phosphorus acquisition and plant growth promotion. *Physiology and Molecular Biology of Plants, 17*(2), 93–103.

Singh, B., & Satyanarayana, T. (2011b). Phytases from thermophilic molds: Their production, characteristics and multifarious applications. *Process Biochemistry, 46*(7), 1391–1398.

Tan, H., Miao, R., Liu, T., Cao, X., Wu, X., Xie, L., … Gan, B. (2016). Enhancing the Thermal Resistance of a Novel Acidobacteria-Derived Phytase by Engineering of Disulfide Bridges S. *Journal of Microbiology and Biotechnology, 26*(10), 1717–1722.

Türk, M., Sandberg, A.-S., Carlsson, N.-G., & Andlid, T. (2000). Inositol hexaphosphate hydrolysis by Baker's yeast. Capacity, kinetics, and degradation products. *Journal of Agricultural and Food Chemistry, 48*(1), 100–104.

Vashishth, A., Ram, S., & Beniwal, V. (2017). Cereal phytases and their importance in improvement of micronutrients bioavailability. *3 Biotech, 7*(1), 1–7.

Xie, Y.-P., Shen, Y.-L., Duan, G.-X., Han, J., Zhang, L.-P., & Lu, X. (2020). Silver nanoclusters: Synthesis, structures and photoluminescence. *Materials Chemistry Frontiers, 4*(8), 2205–2222.

Yao, M. Z., Zhang, Y. H., Lu, W. L., Hu, M. Q., Wang, W., & Liang, A. H. (2012). Phytases: Crystal structures, protein engineering and potential biotechnological applications. *Journal of Applied Microbiology, 112*(1), 1–14.

Zhang, G.-Q., Wu, Y.-Y., Ng, T.-B., Chen, Q.-J., & Wang, H.-X. (2013). A phytase characterized by relatively high pH tolerance and thermostability from the shiitake mushroom Lentinus edodes. *BioMed Research International*.

Zhang, J., Xu, S., & Kumacheva, E. (2005). Photogeneration of fluorescent silver nanoclusters in polymer microgels. *Advanced Materials, 17*(19), 2336–2340.

Zhang, Z., Yang, J., Xie, P., Gao, Y., Bai, J., Zhang, C., … Gao, X. (2020). Characterization of a thermostable phytase from Bacillus licheniformis WHU and further stabilization of the enzyme through disulfide bond engineering. *Enzyme and Microbial Technology, 142*, Article 109679.

Zheng, K., Yuan, X., & Xie, J. (2017). Effect of ligand structure on the size control of mono-and bi-thiolate-protected silver nanoclusters. *Chemical Communications, 53*(70), 9697–9700.